

Meandering bicrystal Josephson junction arrays in a hemispherical Fabry–Perot resonator

This content has been downloaded from IOPscience. Please scroll down to see the full text.

2007 Supercond. Sci. Technol. 20 S413

(<http://iopscience.iop.org/0953-2048/20/11/S22>)

View [the table of contents for this issue](#), or go to the [journal homepage](#) for more

Download details:

IP Address: 130.237.165.40

This content was downloaded on 05/09/2015 at 05:42

Please note that [terms and conditions apply](#).

Meandering bicrystal Josephson junction arrays in a hemispherical Fabry–Perot resonator

M He^{1,2}, A M Klushin¹ and N Klein¹

¹ Institute of Bio- and Nanosystems and CNI-Centre of Nanoelectric Systems for Information Technology, Forschungszentrum Jülich GmbH, D-52428 Jülich, Germany

² Department of Electronics, Nankai University, 300071 Tianjin, People's Republic of China

E-mail: a.klushin@fz-juelich.de

Received 11 June 2007, in final form 24 July 2007

Published 18 October 2007

Online at stacks.iop.org/SUST/20/S413

Abstract

We have explored the coupling mechanism of a millimeter wave radiation to bicrystal Josephson junction arrays embedded in a Fabry–Perot resonator. In order to optimize the system, three-dimensional simulations and relative experiments were performed. By analyzing the results of computer simulations and experiments, we found that the layout of the array and the distance between the array and the plane mirror should minimize the effects on the electrical field E distribution in the fundamental mode of the Fabry–Perot resonator without the sample. In this case, the uniformity of the E field in the bicrystal arrays was demonstrated together with an improvement in the coupling efficiency of the mm wave irradiation to high-temperature superconductor arrays of Josephson junctions.

(Some figures in this article are in colour only in the electronic version)

1. Introduction

One of the most attractive applications of the Josephson effect in superconducting electronics is connected with the development of quantum voltage standards. The principal importance of this application is based on the fact that other physical effects are not known today which could provide a similar accurate representation of the volt. The base of the present voltage standards constitutes series arrays of Josephson junctions (JJs). These applications require thousands of JJs in series, phase-locked to an applied microwave signal. All of the junctions in the array should have very similar parameters, i.e. critical current I_c and normal resistance R_n in the resistively shunted junction (RSJ) model to achieve this goal. Usually niobium junctions working at helium temperatures are applied in such systems [1, 2].

Special interest was generated by the development of programmable voltage standards. Programmable voltage standards have attracted much attention because they can generate a set of precision voltages. This radically changes the comparison scheme and increases the accuracy and speed of calibration. A new type of voltage standard

for fast dc measurements has been recently demonstrated with Nb- and NbN-based Josephson junctions having a nonhysteretic current–voltage characteristic at liquid helium temperature [3–5].

Such nonhysteretic junctions are naturally available in a high-temperature superconductor (HTS) technology. The main advantage of HTSs is the higher operational temperature achievable by low-power cryocoolers. However, in comparison to a low temperature superconductor Josephson junction the spread of parameters of HTS junctions is still very high. Different technologies have been used for studying planar $\text{YBa}_2\text{Cu}_3\text{O}_7$ (YBCO) junctions: the grain-boundary junctions [6], the ramp-type junctions [7] and junctions produced by an ion damage [8–10]. The last technique has been recently used for producing planar MgB_2 Josephson junctions and series arrays containing up to 20 JJs [11].

A very challenging approach developed in Forschungszentrum Jülich GmbH relies on bicrystal arrays with external shunt resistors [12]. Shunted bicrystal HTS Josephson junctions are promising candidates to be used in voltage standard applications. First, they follow the resistively shunted junction (RSJ) model. Second, these junctions have large critical currents and

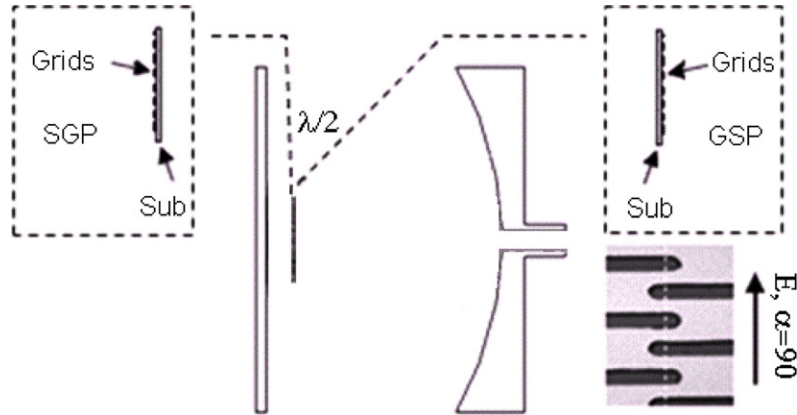


Figure 1. Schematic of the hemispherical Fabry–Perot resonator with the HTS array placed at the half-wavelength distance from the plane mirror. The insets at the top show two different types of irradiation schemes of the HTS arrays in the FP resonator: the HTS array placed facing the spherical mirror is denoted as a grids–substrate–plane mirror (GSP) structure; the HTS array placed facing the plane mirror is denoted as a substrate–grids–plane mirror (SGP) structure. The inset at the bottom right side shows the layout of the HTS array circuit. The grain boundary (GB) is marked as a dashed line. The mutual angle α between the strips and the electric field vector E is 90° .

first current steps at temperatures up to 80 K, and provide stability against noise as well as a large output current. Third, their characteristic voltages, $I_c R$ (where R is the shunted junction resistance), can easily be varied in a practically important range between 20 and 200 μV and enable operating frequencies from 10 to 100 GHz. Finally, a significant enhancement of the packing density of junctions is possible by using a substrate with several grain boundaries and electron-beam patterning.

Shunted bicrystal junctions were fabricated by using Au–YBCO bilayers deposited *in situ* on symmetrical yttrium-stabilized zirconium oxide (YSZ) substrates. With such an array the spread of the junction normal state resistance R is kept at only a few per cent, whereas the spread of the critical current I_c is still of the typical order of 30%. Under these conditions, the individual voltage steps of all N junctions emerge within an overlapping current interval resulting in the occurrence of one single voltage step of a reasonable width (with respect to thermal noise) for the whole array at a voltage $V = Nf/K_J$, where f is the irradiation frequency and $K_J \equiv h/2e$ is the Josephson constant. The maximal number of synchronizing junctions N was equal to 256 [13].

Other important requirements for the formation of stable and wide Shapiro steps is to make a uniform microwave energy coupling over all the junctions. In low-temperature voltage standards, a straight-line series array of Josephson junctions is embedded along either a microstrip line [14], or the center conductor of a coplanar waveguide (CPW) [15], or in both conductors of the slot line [16]. The propagating electromagnetic wave effectively drives the arrays containing up to several thousands of junctions. In contrast, the series array of bicrystal junctions is laid out as a meander line. This prevents the uniform distribution of ac current along such an array. To overcome this drawback the meander array was placed parallel to the usual CPW. This provides parallel feeding of microwave power to all junctions [13]. Microstrip [17] and waveguide resonators were previously explored for irradiation of the JJ array at frequencies below 40 GHz [18].

Recently we suggested and successfully implemented a method of irradiating arrays of high- T_c Josephson junctions

by coupling them to the resonant modes of a millimeter wave Fabry–Perot (FP) resonator [19]. The Fabry–Perot resonator is an open resonator and can resonate at mm wave and even sub-mm wave with a high quality factor [20]. When it works in quasi-basic TEM mode, the electromagnetic field distribution near the plane mirror in a hemispherical FP resonator is similar to the plane wave. It can irradiate uniform power on the Josephson junction arrays. We have achieved a maximum Josephson voltage of 28 mV at 74.4 GHz [21], but the step height was very small for practical applications at only 20 μA .

In this paper, we present the results of simulations and experiments used to study the influences of different layouts of arrays, the distance from the array to the plane mirror and the radius of the curvature of the spherical mirror on the coupling of Josephson junctions to the mm wave radiation in the FP resonator. After the coupling conditions were optimized, the step height was increased by a factor of approximately ten.

2. Fabry–Perot resonator system and high-temperature Josephson junction arrays

The FP resonator was arranged in a hemispherical configuration with plane and spherical mirrors (figure 1). A sample with an array of high-temperature Josephson junctions was placed between the two mirrors, parallel to the plane mirror. The radius of the curvature of the spherical mirror was equal to 25 or 50 mm.

The inset at the bottom right in figure 1 shows the layout of the HTS array circuit. The grain boundary (GB) is marked by a dashed line and is located in the middle of a bicrystal substrate with dimensions $10 \times 10 \text{ mm}^2$. The GB divides the substrate into two equal parts. The metallized parts (light areas at the low right inset of figure 1) are extended over a length of 4 mm and form a grid composed of metal strips. The two sub-grids below and above the GB are connected in the middle of the substrate with the bridges crossing the GB, forming a series array of 580 junctions with a lateral size of 6 mm and the width of each junction is 6 μm . The shunted junctions were fabricated using Au–YBa₂Cu₂O_{2-x} bilayers deposited

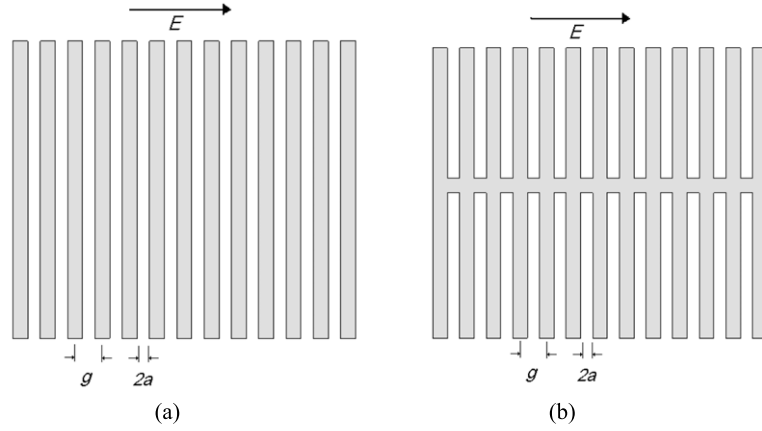


Figure 2. An array of parallel metal strips (a) and a simplified model of the BJJ array (b).

in situ on bicrystal symmetrical yttrium-stabilized zirconium substrates with a misorientation angle of 24° . Details of the deposition process and the technology of shunted GB junctions were published previously [22].

As shown in figure 1, we investigated the influence of the distance d between the array and the plane mirror. We used two different types of irradiation schemes of the HTS arrays in our FP resonator system. In the first case, the HTS array was placed facing the spherical mirror. We denote this case as the grids–substrate–plane mirror (GSP) structure. In the second case, the HTS array was placed facing the plane mirror and is denoted as the substrate–grids–plane mirror (SGP) structure.

3. Simulations and experiments

3.1. Optimization of the distance dependence between the plane mirror and the array

We have stated that our bicrystal Josephson junction (BJJ) array embedded in a FP resonator can be modeled as a thin film grid polarizer [21]. However, recent simulation results and experiments have shown that the grids can work as a thin film grid polarizer under certain special conditions. These are dependent on the distance d , which denotes the distance between the plane mirror and the grids.

As illustrated in figure 2(a), an array of parallel thin film metal strips can be considered a polarizer, when the spacing g of the strips is taken to be significantly less than half a wavelength ($\lambda/2$) and the width of the strips $2a$ is not greater than $\lambda/10$. For an electric field polarized perpendicular to the grid direction, the shunt impedance of the grid is much higher than that of free space, which allows the field to transmit through the grids without any effect [23]. However, our BJJ array is designed differently from typical parallel grids. In simplified form, it can be modeled as shown in figure 2(b). In this model, a thin film strip perpendicular to the grid connects the latter in the middle. It should be noted that the dielectric constant of the substrate in the model was $\varepsilon = 1$. Numerical field simulations of the structures shown in figure 2 were performed with CST Microwave Studio [24].

The influence of the distance between the grids and the plane mirror was explored. First, we found that, without

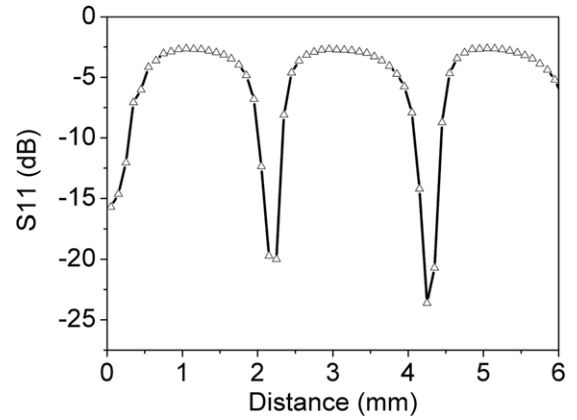


Figure 3. Simulation results of S_{11} at resonance frequency f_R when the distance d between the grid and the plane mirror is changed from 0 to 6 mm.

a sample, the resonance frequency of the FP resonator is equal to $f_R = 72.2$ GHz and the wavelength is about $\lambda \cong 4.15$ mm when the distance between the mirrors is 16.85 mm. Furthermore, the parameter S_{11} was simulated when the grid shown in figure 2(b) was embedded in the resonator. In the simulations, the distance d was changed from 0 to 6 mm. Figure 3 shows that resonance frequency remains as before and is equal to approximately f_R , only when the grid is placed at distances $d \approx N\lambda/2$, where $N = 0, 1, 2, \dots$

To explain this feature, we simulated the electric field distribution when the FP system resonates at quasi- TEM_{00q} mode with the sample placed at distance $d = \lambda/2$ from the plane mirror. The simulation results shown in figure 4 demonstrate the distribution of electric field intensity E in the standing wave formed in the resonator. The contours show different amplitudes of E and inner contours denote higher values. The amplitudes of E inside contours are much larger than the one of the area outside the outermost contours, which is close to zero. From figure 4, it is evident that, for $d \approx N\lambda/2$, the grid is placed at the plane with the minimum electric field intensity E , i.e. the grid has almost no effect on the field distribution in a FP resonator. Under this condition, the quality factor Q of the FP is high as shown in figure 5,

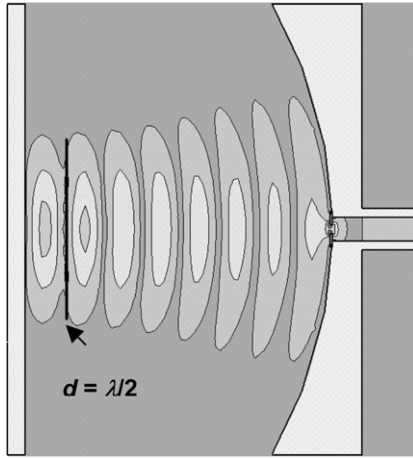


Figure 4. The simulation results demonstrate the distribution of electric field intensity E in the standing wave formed in the resonator. The contours show different amplitudes of E and inner contours denote higher values. The amplitudes of E inside contours are much larger than the one of the area outside the outermost contours, which is close to zero. The grid is placed at a distance $d \approx \lambda/2$ from the plane mirror with the minimum electric field intensity E .

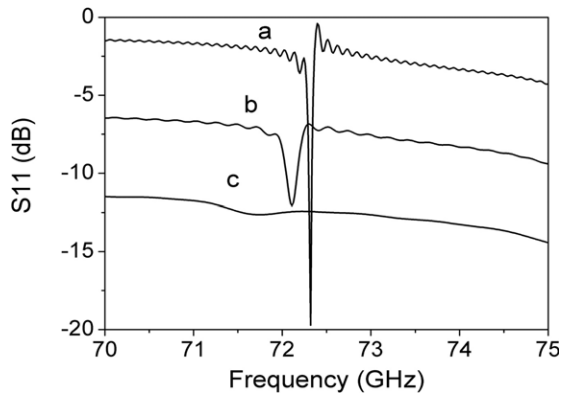


Figure 5. Simulation results of S11 when the grid is placed at a distance equal to: (a) half-wavelength, (c) quarter-wavelength and (b) between a quarter and a half-wavelength from the plane mirror. To show the difference of the S11 results more clearly, curves (b) and (c) are shifted in the vertical axis to -5 dB and -10 dB, respectively.

curve (a). In contrast, if we move the grid to the plane where $d = (2N + 1)\lambda/4$, i.e. maximum electric field intensity, the resonance in the FP resonator will be depressed as shown in figure 5, curve (c). In the intermediate case, when $N\lambda/4 < d < (N + 1)\lambda/4$, the resonance frequency will shift and the Q factor of our FP system will decrease (figure 5, curve (b)) in comparison with curve (a). To show the difference of the S11 results more clearly, curves (b) and (c) are shifted in the vertical axis to -5 dB and -10 dB, respectively.

When the array of the strips is perpendicular to the electric field, the strips in the middle of the grid, as are shown in figure 2(b), are parallel to the electric field. Therefore, the electric field will be reflected by the strips and affect the distribution of the electric field. Only when the grid is placed in planes with $d = N\lambda/2$, with the minimum electrical field intensity will the distribution of the field at these planes remain

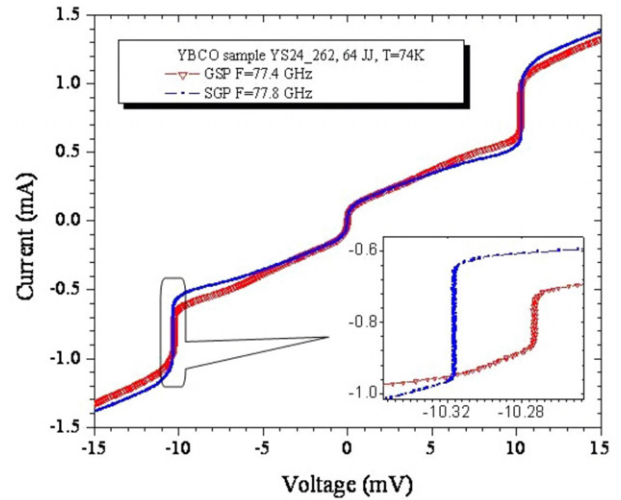


Figure 6. Current–voltage characteristics of the array of 64 BJJs in the GSP and SGP measuring structures. Enlarged portions demonstrate the steps' amplitudes and their steepness.

unaffected by the strips parallel to the electric field due to the small size of the strip and the weak electric field. Our results show that the Josephson circuit should be designed and placed in the resonator in such a way that it minimizes disturbances of the field distribution in the fundamental mode of the FP resonator without the sample. In this case, the optimal coupling between the array and mm wavefield in the resonator can be achieved.

It was also observed that the maximum surface current on the BJJ arrays can be achieved when the grids are located close to the plane mirror at a distance of less than 0.1 mm.

3.2. The influence of different measuring structures

In our previous experiments [21], we employed the GSP structure and placed the sample directly on the plane mirror. In order to couple enough energy into the BJJ arrays, the irradiating microwave power has to be no less than 22 mW at the input of the resonator. If the distance between the sample and the plane mirror is increased and adjusted to an optimal value, the maximum step height can be achieved with a power of about 15 mW. However, the maximum step height was achieved with a power of less than 7 mW in the proposed SGP structure. Experiments show that a larger area of the uniform field can be achieved compared to the GSP structure and thus the step height ΔI_1 was increased from 0.13 to 0.35 mA as shown in figure 6. Moreover, we can move the grids close to the plane mirror only when the SGP structure is used.

3.3. Influence of the radius of curvature of the hemispherical mirror

The simulation and experimental results demonstrate that, if the radius of the curvature of the hemispherical mirror increases, the area of the uniform field will also increase. As shown in figure 7, the step height increases from 0.02 to 0.25 mA when the radius R is changed from 25 to 50 mm for the array with 182 BJJs. More junctions can be synchronized by increasing the radius of the spherical mirror.

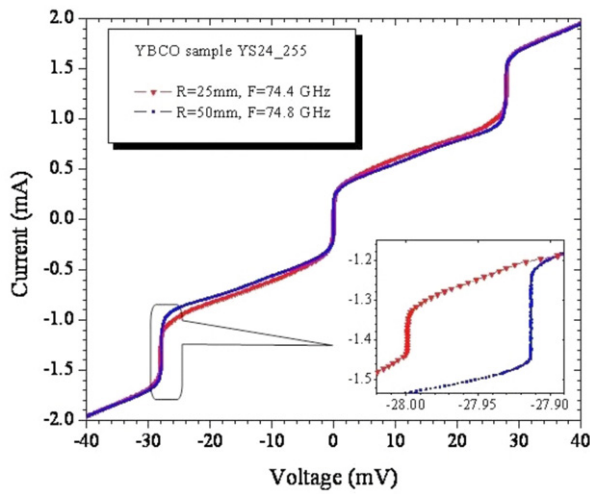


Figure 7. Current–voltage characteristics measured for two different radii of the curvature of the hemispherical mirror with external irradiation. Enlarged portions demonstrate the steps’ amplitudes and their steepness.

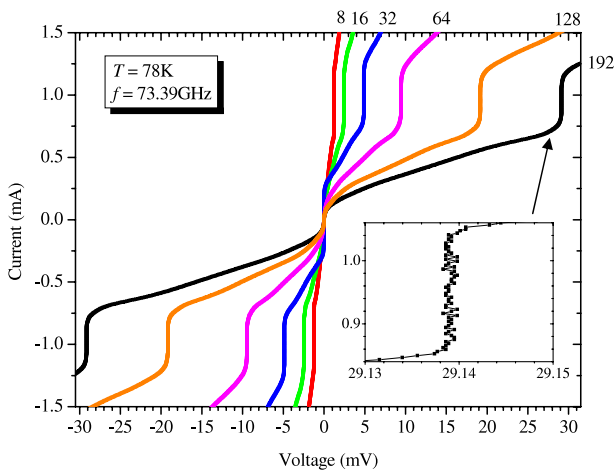


Figure 8. Current–voltage characteristics for six sub-arrays of 8, 16, 32, 64, 128 and 192 junctions measured at $T = 78$ K and irradiation frequency $f = 73.4$ GHz. The enlarged portion demonstrates the step amplitude measured with the resolution $1 \mu\text{V}$ at the voltage of about 29 mV.

3.4. The influence of the number of junctions on the step height

We investigated voltage steps measured for different sub-arrays containing 1, 2, 4, 8, 16, 32, 64, 128 and 192 junctions, respectively. Figure 8 shows the current–voltage characteristics of sub-arrays containing 8 and more junctions measured at 78 K with irradiation frequency of $f = 73.4$ GHz. The Josephson junctions in the arrays had an average critical current of $I_c = 0.55$ mA; the average resistance of one shunted junction was about 0.17Ω . The resulting characteristic frequency f_c was about 50 GHz. The step heights ΔI_1 were measured with a resolution better than $1 \mu\text{V}$. Precision measurements revealed that we achieved more than 29 mV on the sub-array containing 192 junctions with $\Delta I_1 \cong 0.17$ mA. Figure 9 demonstrates the dependence of the step height on

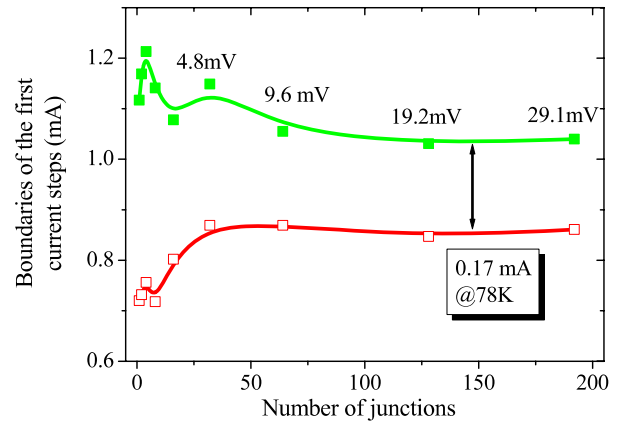


Figure 9. The top (closed squares) and bottom (open squares) boundaries of the first current steps versus the number of junctions in the sub-arrays at $T = 78$ K and irradiation frequency $f = 73.4$ GHz. The lines are drawn to guide the eye. The numbers above the top line correspond to the voltages on the sub-arrays.

the number of junctions in the sub-arrays. In the small arrays the step height is comparable with the critical current and is equal to $\Delta I_1 \cong 0.45$ mA. However, with an increasing number of junctions, the step height decreases and remains approximately constant on sub-arrays, containing more than 60 junctions. The decrease in step height could be caused by the spread of junction parameters (normal resistances and critical currents) and the non-uniformity of the millimeter wave current distribution on the array. We suppose that the last limitation determined by the width of the Gaussian beam in the fundamental mode of the FP resonator could be fixed by further increasing the radius of the curvature and the diameter of the spherical mirror.

4. Conclusion

We investigated the coupling mechanism of millimeter wave radiation to Josephson junction arrays embedded in a wire grid polarizer structure, arranged in a hemispherical FP resonator. The coupling efficiency of the power can be enhanced by placing the array in the half-wavelength plane of the standing wave in the resonator. At the same time, it was demonstrated that the SGP structure is better than the GSP structure because it is not only able to enlarge the area of the uniform field but also increases the power coupling efficiency to the BJJ arrays. We have shown that the area of the uniform field can be increased by enlarging the radius of the curvature of the spherical mirror. In general, our results show that the Josephson circuit should be designed and placed in the resonator in such a way that it minimizes disturbances to the field distribution in the fundamental mode of the FP resonator without the sample. In this case the optimal coupling between the array and mm wave field in the resonator can be achieved.

Arrays with 192 junctions were synchronized and a maximum quantum Josephson voltage equal to 29 mV with the step height 0.17 mA was measured at the temperature 78 K for the first time. Sub-arrays containing a smaller number of junctions were also synchronized at the same frequency. We plan to increase the Josephson voltage further by substantially

increasing the diameter of the spherical mirror by a factor of 3 or 4, which will increase the width of the Gaussian beam in the fundamental mode of the FP resonator and the uniformity of the electric field on the sample. As a result, the number of synchronized junctions will increase. At the same time, increasing the irradiation frequency by a factor of 2 should assist in essentially increasing the output voltage of the HTS arrays.

References

- [1] Hamilton C A 2000 *Rev. Sci. Instrum.* **71** 3611–23
- [2] Niemeyer J 2000 *Supercond. Sci. Technol.* **13** 546–60
- [3] Benz S P, Hamilton C A, Burroughs C J and Harvey T E 1997 *Appl. Phys. Lett.* **71** 1866–9
- [4] Schulze H, Behr R, Kohlmann J, Müller F and Niemeyer J 2000 *Supercond. Sci. Technol.* **13** 1293–6
- [5] Yamamori H, Ishizaki M, Shoji A, Dresselhaus P D and Benz S P 2006 *Appl. Phys. Lett.* **88** 042503–5
- [6] Hilgenkamp H and Mannhart J 2002 *Rev. Mod. Phys.* **74** 485–549
- [7] Heinsohn J-K, Dittmann R, Rodrigues Contreras J, Scherbel J, Klushin A M, Siegel M, Jia C L, Golubov A and Kupryanov M Yu 2001 *J. Appl. Phys.* **89** 3852–60
- [8] Chen K, Cybart S A and Dynes R C 2004 *Appl. Phys. Lett.* **85** 2863–5
- [9] Bergeal N, Grison X, Lesueur J, Faini G, Aprili M and Contour J P 2005 *Appl. Phys. Lett.* **87** 102502–5
- [10] Bergeal N, Lesueur J, Faini G, Aprili M and Contour J P 2006 *Appl. Phys. Lett.* **89** 112515–7
- [11] Cybart S A, Chen K, Cui Y, Li Q, Xi X X and Dynes R C 2006 *Appl. Phys. Lett.* **88** 012509–11
- [12] Klushin A M, Prusseit W, Sodtke E, Borovitskii S I, Amatuni L E and Kohlstedt H 1996 *Appl. Phys. Lett.* **69** 1634–6
- [13] Klushin A M, Weber C, Kohlstedt H, Starodubrovskii R K, Lauer A, Wolff I and Semerad R 1999 *IEEE Trans. Appl. Supercond.* **9** 4158–61
- [14] Niemeyer J, Hinken J H and Kautz R L 1984 *Appl. Phys. Lett.* **45** 478–80
- [15] Benz S P 1995 *Appl. Phys. Lett.* **67** 714–6
- [16] Schubert M, May T, Wende G, Fritzsche L and Meyer H G 2001 *Appl. Phys. Lett.* **79** 1009–11
- [17] Klushin A M, Schornstein S, Kohlstedt H, Wende G, Thrum F and Meyer H G 1997 *IEEE Trans. Appl. Supercond.* **7** 2423–5
- [18] Klushin A M, Goldobin E, Melkov G A, Ivanyuta O N, Egorov Y V, Numssen K and Siegel M 2001 *IEEE Trans. Appl. Supercond.* **11** 944–7
- [19] Klushin A M, Druzhnov D M and Klein N 2006 *J. Phys. Conf. Ser.* **43** 1155–8
- [20] Clarke R N and Rosenberg C B 1982 *J. Phys. E: Sci. Instrum.* **15** 9–23
- [21] Klushin A M, He M, Yan S L and Klein N 2006 *Appl. Phys. Lett.* **89** 232505–7
- [22] Klushin A M, Weber C, Darula M, Semerad R, Prusseit W, Kohlstedt H and Braginski A I 1998 *Supercond. Sci. Technol.* **11** 609–13
- [23] Goldsmith P F 1997 *Quasioptical Systems: Gaussian Beam Quasioptical Propagation and Application* (New York: IEEE Press/Chapman and Hall) p 192
- [24] CST Microwave Studio, Available at: <http://www.cst.com>